The Dynamic Response of Plate with Two Ribs under Impact Load

The Dynamic Response of Plate with Two Ribs under Impact Load

Hiroshi Takano*, Norimitsu Kishi
and Sumio G. Nomachi**

Abstract

Reaction against normal impulsive forces on the midspan of a rectangular acryl plate, which is reinforced by two ribs parallel to its free sides, was measured.

Stress analysis corresponding to the test was carried on by means of dynamic finite strip method.

Initial stress behavior and action of the ribs in the test approximately agree with the numerical results.

1. INTRODUCTION

The response of a plate under dynamic load has importance in many applications. The objective is to keep the plate from undesirable response by all means. Attaching ribs to the plate are a common way of reinforcement.

According to C. Zerner[1], the center of disturbance, the point where the impulse acted, remains stationary until the return of the disturbance reflected from the boundary of the plate. This implys that when the impulsive load acts between the ribs, their action associated with the plate should differ from what is supposed to be in case of statics.

The present investigation was undertaken to gain insight into the initial response of the rectangular plate with ribs, under the normal impulse by way of test and analysis. The rectangular plate with two ribs parallel to its pair of free sides made of acryl resine is used, and the stress analysis is performed by means of dynamic finite strip method[2].

* Structure Departure of Civil Engineering Laboratory, Central Research Institute of Electric Power Industry, Abiko, Chiba.

** Departure of Civil Engineering, Hokkaido University, Sapporo.

2. EXPERIMENTS

Figure 1 shows an outline of the experimental set up and a flow chart of the measurement. Experimental technique is almost similar to the one what we used for the beam impact problems[3),4)]. The boundary conditions of the plate are two opposite sides free and the other sides hinged. A rod is set on the midspan of the plate, which is impacted

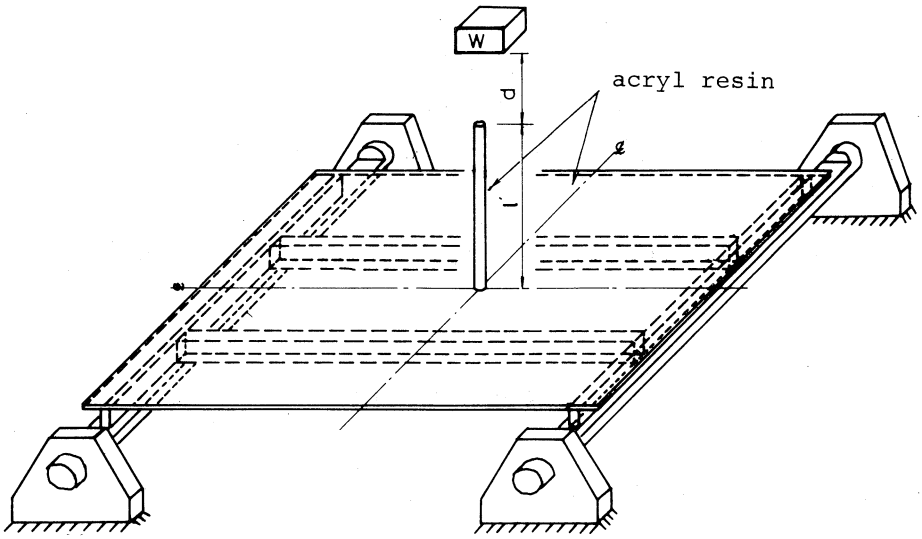

(a) experimental equipment

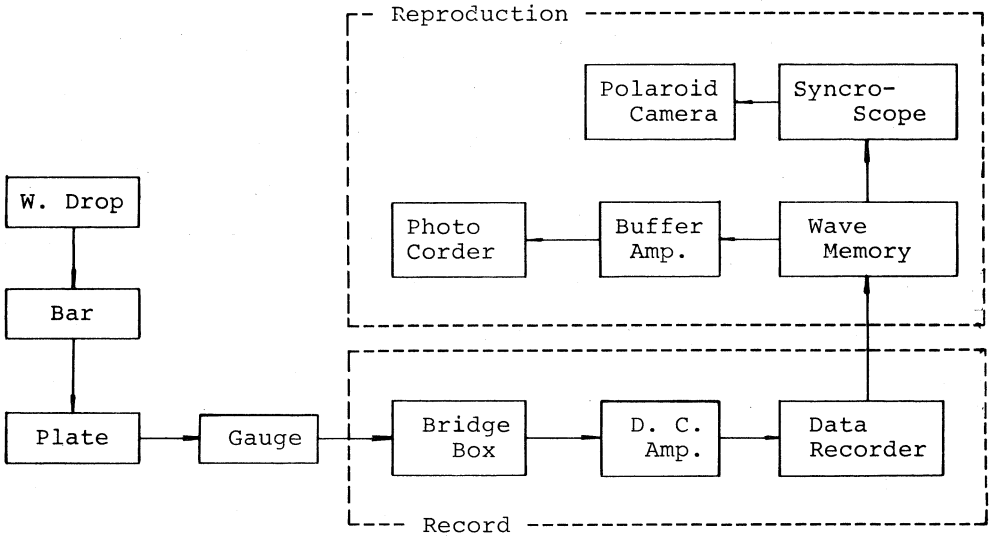

(b) measurement block diagram

Fig. 1 Experimental set up

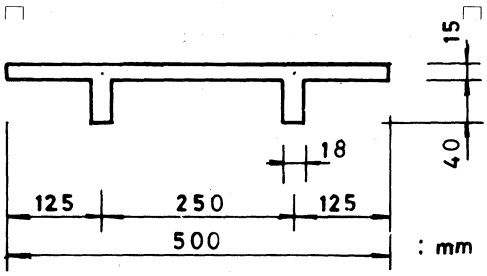

Span Length $l = 100$ cm
Elastic Rod $l = 50$ cm
$\phi = 30$ mm
Drop Weight $W = 1.9$ Kg
$d = 30$ cm
Acryl resin $E = 30000$ Kg/cm^2
$\nu = 0.38$
$\rho = 1.18$ g/cm^3

Fig. 2 Specifications of the plate with two ribs and elastic rod

through the rod by a dropping weight. The variation of impact intensity is observed by a strain gauge at the bottom of the rod and measured impact will be applied to the impact load on the plate in case of numerical calculation.

Strains on the surface of the plate are measured by means of one gauge method, that is a foil strain gauge whose length is 1 mm and resistance 120 Ω. In order to record the high frequency components, a D. C. Amp. that can measure up to 20 KHz was used and the measured data were recorded by a wide band data recorder, and the strains were stroed in Wave Memory, so that we could reproduce and magnify them any optional time span.

By making use of symmetry of the strain distribution, we limited the measurement to a quarter or a half of the plate. The specifications of the plate with two ribs and the loading rod are shown in Figure 2. The impact was produced by 1.9 kg weight dropped for 30 cm above the loading rod.

Symmetrical loading is for the case when the impact load acts on the midpoint of plate, and eccentrical loading for the case when the impact load acts on the central point of one rib, respectively.

3. EXPERIMENTAL RESULTS

Figures 3 and 4 show the variations of strains with time for the symmetrical and ec-

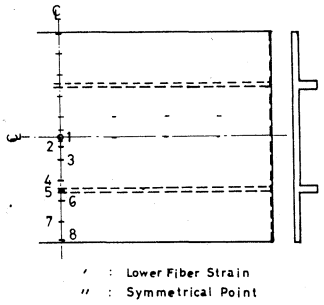

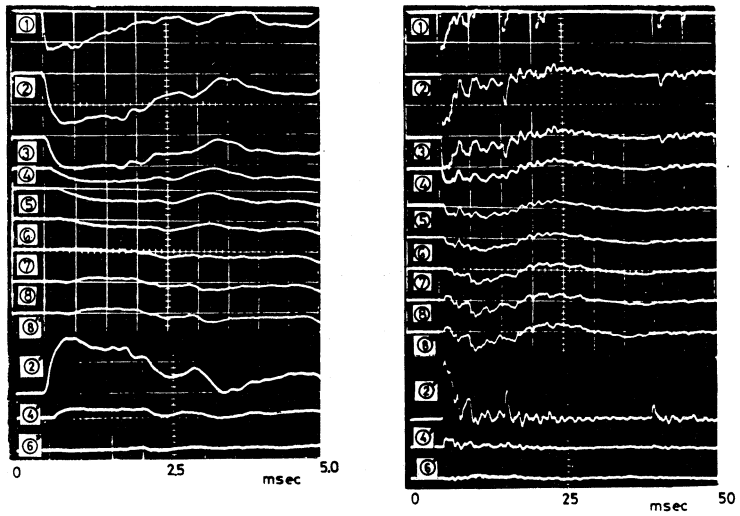

(a) variation of longitudinal strain

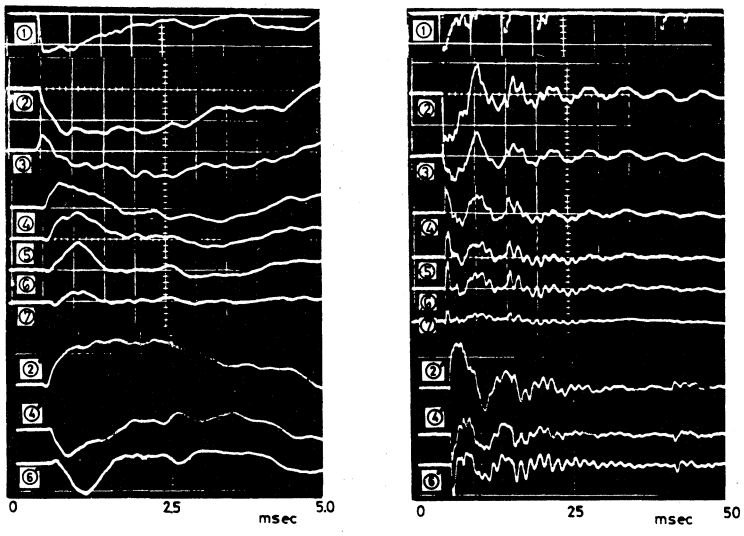

(b) variation of transversal strain

Fig. 3 Variation of strain on top surface of plate in case of symmetrical loading

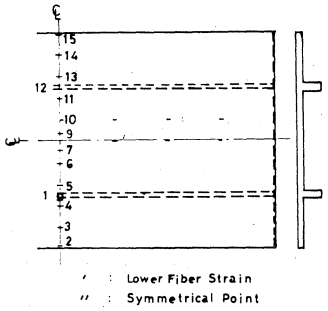

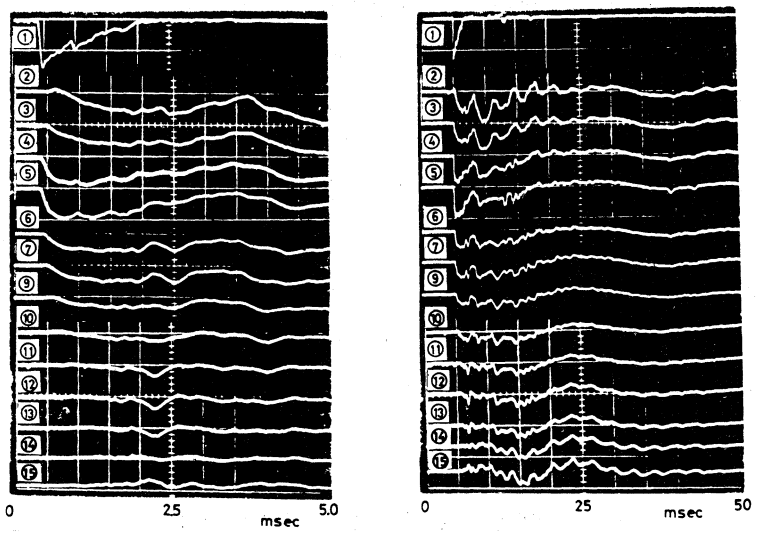

(a) variation of strain on top surface of plate

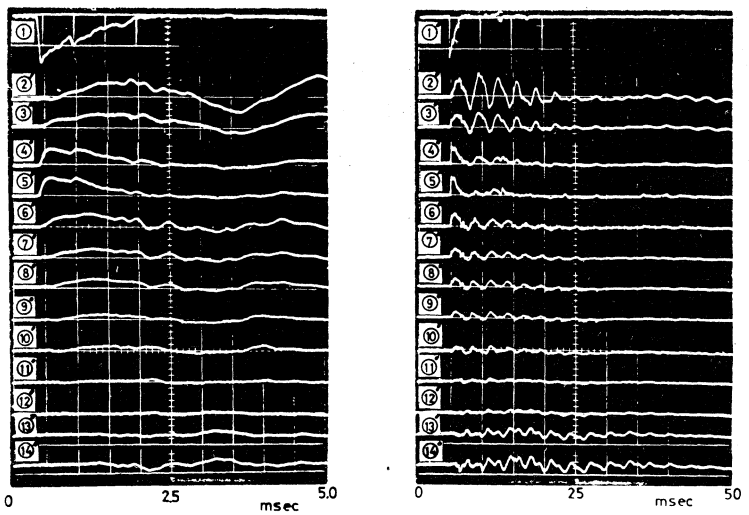

(b) variation of strain on bottom surface of plate

Fig. 4 Variation of longitudinal strain in the plate in case of eccentrical loading

centrical loading, respectively. The impact strain in the rod is illustrated in Figure 3 by ①, whose curve is a triangular distribution with the duration of about 2.5 msec.

The variation of strains at the incident moment of impact in Figure 3 (a), shows that the strain wave front advances in concentric way about the speed of shear velocity. The strain gauges ②, ④ and ⑥, which are glued on top and bottom surfaces of the plate, give all symmetric pattern at the incident moment before 5 msec, as shown in Figure 3 (a). This implys that the ribs do not play a part of the structure and the plate behaves as a plane plate. For the time being, the strains vary in a manner of the natural vibration of the composite structure of plate and ribs, and the maximum response takes place at the very beginning as shown in Figure 3 (a). It is very much like in case of impact of infinite beam due to bending.

The strain measurement when the impact load acts on a central point of one rib is illustrated in Figure 4. Comparing, for instance, two curves of ⑤ with each other, we can see that the one for the top surface clearly differs from the other for the bottom surface. This implys that the composite action of the rib may occur from the beginning of impact. For the time being, the response rapidly moves to the natural vibration of the plate with two ribs.

4. THEORETICAL ANALYSIS

Long sizes of a strip element are denoted by i and j nodes, displacements in the x-, y- and z-directions by u, v and w, and rotation about x axis by θ, as shown in Figure 5.

The function for w, θ may be expressed by cubic variation of y and for u, v linear of y in the narrow direction of the strip element.

Thus,

$$u=u^{(i)}u_i+u^{(j)}u_j \qquad \cdots\cdots (1)$$

$$v=v^{(i)}v_i+v^{(j)}v_j \qquad \cdots\cdots (2)$$

$$w=w^{(i)}w_i+w^{(j)}w_j+\theta^{(i)}\theta_i+\theta^{(j)}\theta_j \qquad \cdots\cdots (3)$$

in which

$$\left.\begin{aligned} &u^{(i)}=v^{(i)}=1-\eta \\ &u^{(j)}=v^{(j)}=\eta \\ &w^{(i)}=1-3\eta^2+2\eta^3 \end{aligned}\right\} \qquad \cdots\cdots (4)$$

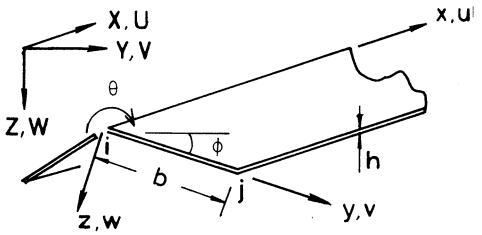

Fig. 5 One strip element

$$w^{(j)}=3\eta^2+2\eta^2$$
$$\theta^{(i)}=b(\eta-2\eta^2+3\eta^3)$$
$$\theta^{(j)}=b(-\eta^2+\eta^3)$$

where $\eta=y/b$. The position of the displacements are identified by the suffix i and j.

The Galerkin's method[5] will be applied to equilibrium equations of in-plane and out-plane forces with the weight function $u^{(k)}$, $v^{(k)}$, $w^{(k)}$ and $\theta^{(k)}$ ($k=i$ or j) ;

$$\int_0^b\left(\frac{\partial\sigma x}{\partial x}+\frac{\partial\tau xy}{\partial y}-\rho\frac{\partial^2 u}{\partial t^2}\right)u^{(k)}dy=0 \qquad \cdots\cdots (5)$$

$$\int_0^b\left(\frac{\partial\tau xy}{\partial x}+\frac{\partial\sigma y}{\partial y}-\rho\frac{\partial^2 v}{\partial t^2}\right)v^{(k)}dy=0 \qquad \cdots\cdots (6)$$

$$\int_0^b\left(\frac{\partial^2 Mx}{\partial x^2}+2\frac{\partial^2 Myx}{\partial x\partial y}+\frac{\partial^2 My}{\partial y^2}-\rho h\frac{\partial^2 w}{\partial t^2}+p\right)w^{(k)}dy=0 \qquad \cdots\cdots (7)$$

$$\int_0^b\left(\frac{\partial^2 Mx}{\partial x^2}+2\frac{\partial^2 Myx}{\partial x\partial y}+\frac{\partial^2 My}{\partial y^2}-\rho h\frac{\partial^2 w}{\partial t^2}+p\right)\theta^{(k)}dy=0 \qquad \cdots\cdots (8)$$

and integrating by parts eq. (5)−(8) with Hooke's law, we find the equations between the displacements and the forces on the normal line i and j. Then applying finite Fourier transforms, and taking the natural boundary conditions for $x=0$ and l, we have the stiffness relation as follows :

$$[K]\{\bar{S}m[\delta]\}+[M]\frac{\partial^2}{\partial t^2}\{\bar{S}m[\delta]\}=\{\bar{S}m[f]\}+\{\bar{S}m[p]\} \qquad \cdots\cdots (9)$$

where

$$\{\bar{S}m[\delta]\}=[\,Cm[u_i]\,Sm[v_i]\;Sm[w_i]\;Sm[\theta_i]$$
$$Cm[u_j]\,Sm[v_j]\;Sm[w_j]\;Sm[\theta_j]\,]^T$$
$$\{\bar{S}m[f]\}=[\,Cm[T_i]\,Sm[S_i]\;Sm[Q_i]\;Sm[M_i]$$
$$Cm[T_j]\,Sm[S_j]\;Sm[Q_j]\;Sm[M_j]\,]^T$$
$$Cm[u]=\int_0^l u\cos\frac{m\pi}{l}xdx,\qquad Sm[v]=\int_0^l v\sin\frac{m\pi}{l}xdx$$

$$T=h\tau xy, \quad S=h\sigma y, \quad Q=\frac{\partial My}{\partial y}+2\frac{\partial Myx}{\partial x}, \quad M=My$$

$m=1, 2, 3,\ldots$

in which $[K]$, $[M]$ are stiffness and mass matrices, $\{Sm[p]\}$ is external force vector by nodal loads. Thus, they are rewritten in the following forms:

$$[K]=GhVp^2\begin{bmatrix} A1 & A3 & & 0 & & A2 & A4 & & 0 & \\ & A5 & & & & -A4 & A6 & & & \\ & & B1 & B3 & & & & B2 & B4 & \\ & & & B5 & & 0 & & -B4 & B6 & \\ & & & & A1 & -A3 & & & & \\ & & & & & A5 & & 0 & & \\ & & & & & & B1 & -B3 & & \\ \text{Symm.} & & & & & & & B5 & & \end{bmatrix}$$

$$[M]=\rho h\begin{bmatrix} C1 & 0 & & 0 & & C2 & 0 & & 0 & \\ & C1 & & & & 0 & C2 & & & \\ & & D1 & D3 & & & & D2 & D4 & \\ & & & D5 & & 0 & & -D4 & D6 & \\ & & & & C1 & 0 & & & & \\ & & & & & C1 & & 0 & & \\ & & & & & & D1 & -D3 & & \\ \text{Symm.} & & & & & & & D5 & & \end{bmatrix} \quad \{Sm[p]\}=Sm[p]\begin{Bmatrix} 0 \\ 0 \\ - \\ E1 \\ E2 \\ \cdots \\ 0 \\ 0 \\ - \\ E1 \\ -E2 \end{Bmatrix}$$

where

$$A1=\frac{b}{3}\left(\frac{m\pi}{l}\right)^2+\frac{1}{bVp^2} \qquad B1=rp^2\left\{\frac{13}{35}\left(\frac{m\pi}{l}\right)^4 b+\frac{12}{5b}\left(\frac{m\pi}{l}\right)^2+\frac{12}{b^3}\right\}$$

$$A2=\frac{b}{6}\left(\frac{m\pi}{l}\right)^2-\frac{1}{bVp^2} \qquad B2=rp^2\left\{\frac{9}{70}\left(\frac{m\pi}{l}\right)^4 b-\frac{12}{5b}\left(\frac{m\pi}{l}\right)^2-\frac{12}{b^3}\right\}$$

$$A3=\frac{-1+3\nu}{4}\left(\frac{m\pi}{l}\right) \qquad B3=rp^2\left\{\frac{11b^2}{210}\left(\frac{m\pi}{l}\right)^4+\left(\nu+\frac{1}{5}\right)\left(\frac{m\pi}{l}\right)^2+\frac{6}{b^2}\right\}$$

$$A4=-\frac{1+\nu}{4}\left(\frac{m\pi}{l}\right) \qquad B4=rp^2\left\{-\frac{13b^2}{420}\left(\frac{m\pi}{l}\right)^4+\frac{1}{5}\left(\frac{m\pi}{l}\right)^2+\frac{6}{b^2}\right\}$$

$$A5=\frac{1-\nu}{6}\left(\frac{m\pi}{l}\right)^2 b+\frac{1}{b} \qquad B5=rp^2\left\{\frac{b^3}{105}\left(\frac{m\pi}{l}\right)^4+\frac{4b}{15}\left(\frac{m\pi}{l}\right)^2+\frac{4}{b}\right\}$$

$$A6=\frac{1-\nu}{12}\left(\frac{m\pi}{l}\right)^2 b-\frac{1}{b} \qquad B6=rp^2\left\{-\frac{b^3}{140}\left(\frac{m\pi}{l}\right)^4-\frac{b}{15}\left(\frac{m\pi}{l}\right)^2+\frac{2}{b}\right\}$$

$$C1=\frac{b}{3} \quad C2=\frac{b}{6} \qquad D1=\frac{13}{35}b \quad D2=\frac{9}{70}b \quad D3=\frac{11}{210}b^2$$

$$E1=\frac{b}{2} \quad E2=\frac{b^2}{12} \qquad D4=-\frac{13}{420}b^2 \quad D5=\frac{1}{105}b^3 \quad D6=-\frac{1}{140}b^3$$

in which $Vp=\sqrt{2/(1-\nu)}$, $rp=h/\sqrt{12}$, and G and ν denote shear modulus and Pisson's ratio.

In order to analyze, the stresses and the displacements in a whole structure, we must transform local coordinate of each strip element into global one. By making use of the matrix $[T]$ in between local and global coordinates, the forces, the displacements and the loads are transformed by following equations :

$$\left.\begin{aligned}&\{\bar{S}m[F]\}=[T]\{\bar{S}m[f]\}\\&\{\bar{S}m[\Delta]\}=[T]\{\bar{S}m[\delta]\}\\&\{\bar{S}m[P]\}=[T]\{\bar{S}m[p]\}\end{aligned}\right\} \quad \cdots\cdots(10)$$

where

$$[T]=\begin{bmatrix}L & 0\\ 0 & L\end{bmatrix} \quad \text{with} \quad [L]=\begin{bmatrix}1 & 0 & 0 & 0\\ 0 & \cos\phi & \sin\phi & 0\\ 0 & -\sin\phi & \cos\phi & 0\\ 0 & 0 & 0 & 1\end{bmatrix} \quad \cdots\cdots(11)$$

ϕ = angle of the element by global coordinate (clockwise positive) as shown in Figure 5.

Thus, the dynamic equations of concerning the whole structure can be expressed by

$$[Kst]\{\bar{S}m[\Delta st]\}+[Mst]\frac{\partial t}{\partial t^2}\{\bar{S}m[\Delta st]\}=\{\bar{S}m[Fst]\}+\{\bar{S}m[Pst]\} \quad \cdots\cdots(12)$$

By letting $\{\bar{S}m[Fst]\}=0$, $\{\bar{S}m[Pst]\}=0$ in eq. (12), eigen values and corresponding mode vectors may be found out. Thus obtained mode matrix $[\Phi]$ together with normal coordinate vector $\{Sm[\Psi]\}$ lead to the relation :

$$\{\bar{S}m[\Delta st]\}=[\Phi]\{\bar{S}m[\Psi]\} \quad \cdots\cdots(13)$$

Substituting eq. (13) into eq. (12) and considering the orthogonality of matrix and Rayleigh damping effect hr, we obtain the equation of motion for the r-th eigen value ωr as follows.

$$\bar{S}m[\ddot{\Psi}r]+2\omega rhr\bar{S}m[\dot{\Psi}r]+\omega r^2\bar{S}m[\Psi r]=Pr/Mr. \quad \cdots\cdots(14)$$

where

$$Mr=\{\Phi r\}^T[Mst]\{\Phi r\}, \qquad Pr=\{\Phi r\}^T\{\bar{S}m[Fst]+\bar{S}m[Pst]\}$$

$\{\bar{S}m[\Psi]\}$ yields $\{\bar{S}m[\Delta st]\}$ through eq. (13). The nodal displacements and forces are ob-

tained by means of inverse finite Fourier transforms.

5. COMPARISON OF THEORETICAL AND TEST RESULTS

The numerical calculations on the two ribs plate, were performed taking 51 terms of the Fourier series. The structure was divided into 14 and 27 strip elements for the symmetrical and eccentrical loading respectively.

The variation of impact load were assumed to be triangular as shown by ① in Figures 3 and 4.

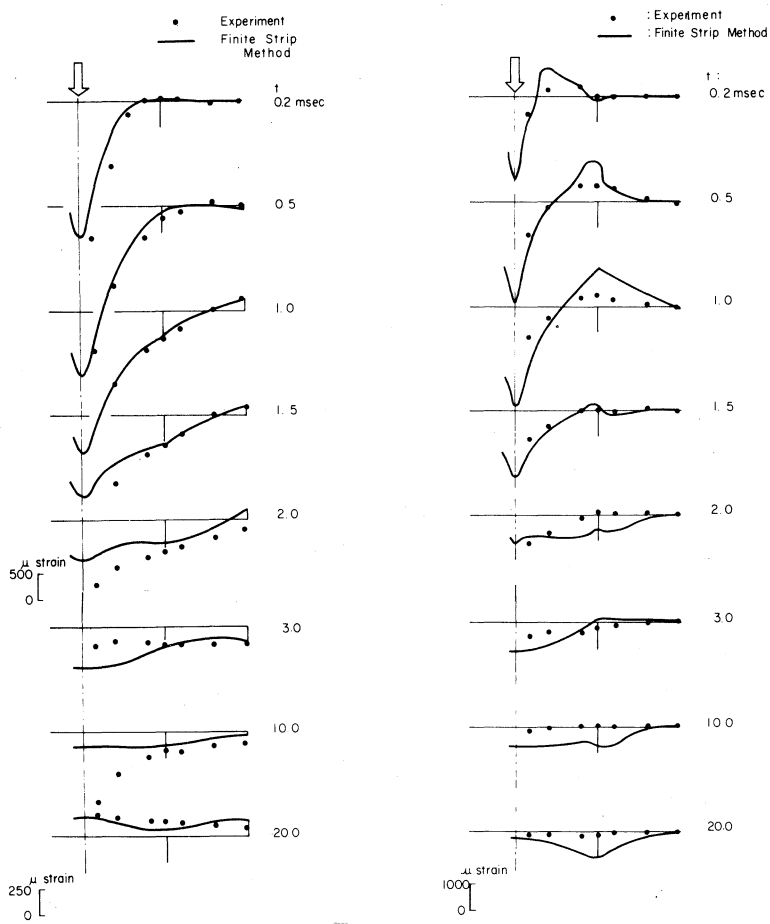

(a) longitudinal strain response (b) transversal strain response

Fig. 6 Comparison of theoretical and experimental strain mode variation over cross section on top surface of plate at midspan in case of symmetrical loading

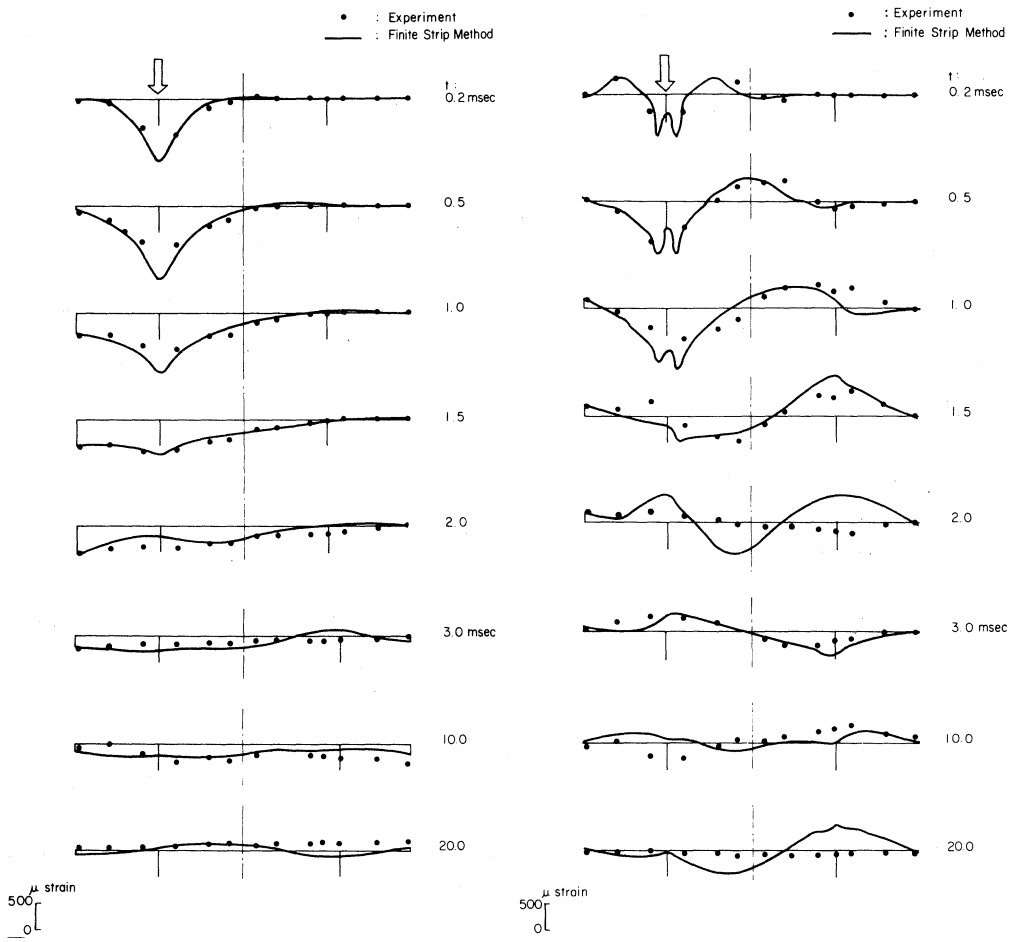

(a) longitudinal strain response (b) transversal strain response

Fig. 7 Comparison of theoretical and experimental strain mode variation over cross section on top surface of plate at midspan in case of eccentrical loading

The measured and analyzed longitudinal and transversal strain distributions over the central cross section at certain time are shown in Figures 6 and 7 for the symmetrical and eccentrical loading, respectively. In both cases, the analytical results may agree with experimental ones very well. This may indicate that the finite strip method is adequately apply for elastic impact problem of folded plate structures.

We can see that the stress wave propagates in transversal as well as longitudinal directions. In the beginning of the impact, the two ribs do not act as composite members and in long time range the ribs get in cooperation with the plate and the whole structure vibrates according to its fundamental mode.

We can also recognize that the wave propagates in the transverse direction from Figure 7. The unloaded rib does not seem to work as a reinforcing member at the incident of impact, whereas the loaded rib then may bears the most impact load.

6. CONCLUTION

Investigating the measured strains in the plate with two ribs from the beginning of impact to the time when the lowest plate vibration occured, with the analyzed strains corresponding to the test, we have the following remark.

(1) The plate with two ribs not behave as the composite structure before the reflectd wave returns from the boundary. The plate responds as a plane plate at the incident of impact which acts on the portion between the ribs. When the impact load acts on one of the ribs, the rib only bears the load at the very beginning of impact.

(2) The finite strip method of stress analysis may deal with the impact problem of folded plate structures.

7. REFERENCES

1) Zener, C., The intrinsic inelastcity large plates. Physical review, Vol. 59 (1941), pp. 669–673.

2) Nakamura, H., Dynamic analysis of thin-walled beams considering cross sectional deformations. J. S. C. E., Vol. 223 (1974), pp. 11–22.

3) Takano, H., Kishi, N. and Nomachi, S. G., On dynamic behavior of beams with rectangular section under impact load. Theoretical & Applied Mech., Vol. 28 (1980), pp. 369–378.

4) Takano, H., Nomachi, S. G. and Kishi, N., On the bending impulse of simple supported composite beams. Theoretical & Applied Mech., Vol. 29 (1981), pp. 213–223.

5) Okumura, T. and Sakai, F., An approach to statical analysis of three-dimensional structures cosisting of thin flat plates and its applications. J. S. C. E., Vol. 176 (1970), pp. 43–59.